A Fractional Physics-Informed Neural Network with Ensemble Learning for Dengue Forecasting

Harshit[0000−0002−6536−4978] and Priyanka Harjule[0000−0002−3481−5764]

Department of Mathematics, Malaviya National Institute of Technology Jaipur, Jaipur 302017, India
kharshit619@gmail.com and priyanka.maths@mnit.ac.in

Abstract. Background. The long-term memory of the disease dynamics and seasonal forcing due to climatic impacts, along with the delayed responses, have made it difficult to accurately predict dengue outbreaks. Traditional compartmental models are based on the Markovian assumption, and the data-driven models may not be easily interpretable from an epidemiological perspective. Fractional calculus provides a sound framework to endow models with memory; nevertheless, combining fractional methods with machine learning techniques requires special attention.

Methods. A fractional physics-informed neural network (FPINN) based on a SEIR-SI dengue compartment model, using Caputo fractional derivatives and L1 time discretization, is proposed. An ensemble averaging of five pre-defined fractional orders is simulated to model the memory effects. The model includes multi-scale temporal encoding, residual learning, and time-dependent transmission rates adjusted by environmental factors. The adaptive physics loss weighting balances the physics and data loss functions during training.

Results. The effectiveness of the proposed approach is demonstrated using the weekly dengue incidence data from San Juan, Puerto Rico. The fixed-α FPINN ensemble achieves strong predictive performance, with a test-set MAE of 6.25 and an R^2 of 0.896. In comparison to data-driven time series baselines, the ensemble reduces the MAE by 29.1% relative to a Long Short-Term Memory (LSTM) model and by 36.2% as compared to a Temporal Convolutional Network (TCN). It also improves MAE by 6.7% over the best individual fixed-α model ($\alpha = 0.95$). In addition to enhanced accuracy, the ensemble provides well-calibrated predictive uncertainty as well.

Conclusion. The findings suggest that the combination of fractional-order memory with physics-informed learning constitutes an effective and interpretable model for dengue forecasting. The fixed-α ensemble FPINN method improves the stability, accuracy, and uncertainty estimation, providing a sound model for epidemic forecasting.

Keywords: Physics Informed Neural Networks(PINNs) · Susceptibles-Exposed-Infected-Recovered(SEIR) model · Ensemble learning · Dengue forecasting · Data-driven epidemiological models

ICCS Camera Ready Version 2026
To cite this paper please use the final published version:
DOI: 10.1007/978-3-032-29912-3_30

1 Introduction

Dengue is one of the most important vector-borne viral diseases in the world. According to the World Health Organization, there are 100-400 million cases of dengue infection every year in more than 100 countries [19]. This arbovirus is mainly transmitted by the Aedes aegypti and Aedes albopictus mosquitoes and shows complex spatiotemporal patterns due to complex interactions between the human host population, the mosquito vector population, and environmental factors such as the temperature, humidity, and rainfall [9,11]. The rapid spread of dengue infection in the world and the impact of climate change on the habitats of the mosquitoes emphasize the need for accurate forecasting models [11].

The traditional mathematical models of dengue disease transmission have mostly relied on compartmental models, for example, the Susceptible-Exposed-Infectious-Recovered (SEIR) model for humans and the Susceptible-Infectious (SI) model for mosquitoes [5]. Although these models have offered a basic understanding, they have challenges in including the memory effects of the previous epidemic conditions that continue to affect the present transmission rates, thus neglecting the Markovian property of the classical ODE models. The dengue epidemic data often show long-range correlations which are generally not captured by the integer-order models [15,2].

Fractional calculus is characterized by its non-local operators and power-law kernels, which provide a mathematically sound setting for overcoming integer order model limitations by introducing memory and anomalous behavior into epidemiological models [13]. The Caputo fractional derivative has been found to be very useful in epidemiological modeling due to its well-posed initial conditions and compatibility with real-life data [3]. Recent advances have provided well-posedness results, stability studies, as well as numerical schemes for fractional epidemiological models [6]. Empirical studies have shown that the fractional epidemic models can produce better statistical fits of disease incidence than their integer-order counterparts for many infectious diseases, such as hepatitis B [18], HIV [7], malaria [1], and dengue [17].

However, despite the benefits, there are several issues that may arise during the implementation process. The non-local property of fractional derivatives makes their discretization more complex, which is then achieved through methods like the L1 scheme for Caputo derivatives [8].

Physics-Informed Neural Networks (PINNs) is a recent method of modeling infectious diseases through a combination of machine learning and compartmental models data. PINNs do not merely use training data as in regular neural networks, but regularize the loss function with the underlying ordinary differential equations (ODEs) of infectious disease dynamics in the first place [14,10,16]. This method enables the model to comply with physical laws, e.g., conservation of populations, yet learn using sparse or noisy data. The recent development in PINNs is the introduction of fractional PINNs (FPINNs). These models utilize the power of fractional calculus to simulate memory and non-local processes inherent to the infectious disease but typically ignored by integer-order models (PINNs) [12]. As an example, Zinihi et al. introduced a fractional SEIRD PINN,

ICCS Camera Ready Version 2026
To cite this paper please use the final published version:
DOI: 10.1007/978-3-032-29912-3_30

which learns the order of the memory (fractional) and epidemiological parameters using noisy COVID-19 and Mpox data that are better than integer-order models in terms of predictive accuracy [20].

Even with these improvements, there are still some research gaps at the intersection of fractional calculus, physics-informed machine learning, and dengue epidemiology that can be filled:

Gap 1 Limited Integration of Fractional Calculus with Modern Machine Learning Frameworks: Although both fractional epidemic models and PINNs have shown individual potentials, their integration is mostly unexamined. This gap provides an opportunity to utilise the complementary strengths of both methodologies.

Gap 2 Simplified Treatment of Time-Varying Transmission Dynamics: Traditional fractional models often assume either constant transmission rates or simple periodic forcing functions that do not take into account the complex and nonlinear dependence of dengue transmission on the environmental factors, human behavior, and intervention measures.

Gap 3 Limited Exploration of Ensemble Methods in disease FPINNs: Although ensemble averaging techniques have shown to be successful for uncertainty estimation, their use in fractional systems has not been investigated extensively yet. The relationship between ensemble diversity, fractional order uncertainty, and prediction accuracy is an area of research that needs to be explored.

This study addresses the identified research gaps through the following interrelated contributions:

1. **FPINN Framework for Dengue Forecasting**: A fractional physics–informed neural network (FPINN) framework is proposed that incorporates Caputo fractional derivatives with L1 discretization to model the memory effects in dengue transmission dynamics. The proposed framework maintains the mechanical structure of a compartmental SEIR-SI model while also utilising neural networks for data-driven forecasting.
2. **Ensemble Modeling with different Fractional Orders**: Various FPINN models are constructed using distinct, pre-specified fractional orders and trained independently. The ensemble aggregation of all models improves the predictive performance while also mitigating sensitivity to fractional-order selection and enables uncertainty-aware forecasting without dependence on direct fractional-order estimation.
3. **Comprehensive Empirical Validation**: The proposed model is validated using multi-year dengue surveillance data from Puerto Rico. The ensemble FPINN approach is systematically compared against integer-order PINNs as well as time series baseline models such as LSTM (Long Short Term Memory), and Temporal Convolutional Network (TCN) by a variety of performance metrics, showcasing improved forecasting accuracy and generalization.

The remaining sections of the article are organized as follows. Section 2 presents the mathematical formulation of the fractional SEIR-SI model and de-

ICCS Camera Ready Version 2026
To cite this paper please use the final published version:
DOI: 10.1007/978-3-032-29912-3_30

tails of the proposed FPINN architecture. Section 3 presents the comprehensive experimental results on dengue surveillance data, which also include the comparison with baseline models and ensemble averaging studies. Section 4 discusses the implications, limitations of the work, along with the conclusion, and future research directions.

1.1 Mathematical Preliminaries

Definition 1 (Caputo fractional Derivative). *Let $f \in C^1([0,T])$ and $\alpha \in (0,1]$. The Caputo fractional derivative of f is defined as [13]*

$$^{C}D_t^{\alpha} f(t) = \frac{1}{\Gamma(1-\alpha)} \int_0^t \frac{f'(\tau)}{(t-\tau)^{\alpha}}\, d\tau, \tag{1}$$

where $\Gamma(\cdot)$ denotes the Gamma function.

Definition 2 (L1 discretization scheme). *Let $t_n = n\Delta t$, $n = 0, \ldots, N$, with time step $\Delta t > 0$. The L1 approximation of the Caputo derivative* (1) *at t_n is:*

$$^{C}D_t^{\alpha} f(t_n) \approx D_{\Delta t}^{\alpha} f(t_n) := \frac{\Delta t^{-\alpha}}{\Gamma(2-\alpha)} \sum_{j=0}^{n-1} b_j^{(\alpha)} \big(f(t_{n-j}) - f(t_{n-j-1})\big), \tag{2}$$

where $b_j^{(\alpha)} = (j+1)^{1-\alpha} - j^{1-\alpha}$ for $j = 0, 1, \ldots, n-1$.

2 Model Formulation and Methodology

A SEIR-SI dengue transmission compartment model describing the interaction between human and mosquito populations is considered. The human population is divided into susceptible $S(t)$, exposed $E(t)$, infectious $I(t)$, and recovered $R(t)$ classes, while the mosquito population is divided into susceptible $S_v(t)$ and infectious $I_v(t)$ classes.

To incorporate memory effects and anomalous temporal dynamics, all state variables are governed by Caputo fractional derivatives of order $\alpha \in (0,1]$. The description of model parameters is given in Table 1.

The fractional SEIR–SI model is given by:

$$^{C}D_t^{\alpha} S(t) = \mu_H - \beta_H(t)S(t)I_v(t) - \mu_H S(t), \tag{3a}$$

$$^{C}D_t^{\alpha} E(t) = \beta_H(t)S(t)I_v(t) - \sigma_H E(t) - \mu_H E(t), \tag{3b}$$

$$^{C}D_t^{\alpha} I(t) = \sigma_H E(t) - \gamma_H I(t) - \mu_H I(t), \tag{3c}$$

$$^{C}D_t^{\alpha} R(t) = \gamma_H I(t) - \mu_H R(t), \tag{3d}$$

$$^{C}D_t^{\alpha} S_v(t) = \mu_V - \beta_V(t)S_v(t)I(t) - \mu_V S_v(t), \tag{3e}$$

$$^{C}D_t^{\alpha} I_v(t) = \beta_V(t)S_v(t)I(t) - \mu_V I_v(t). \tag{3f}$$

ICCS Camera Ready Version 2026
To cite this paper please use the final published version:
DOI: 10.1007/978-3-032-29912-3_30

Table 1. Epidemiological parameters for the fractional SEIR–SI dengue model

Parameter	Description	Typical ranges for dengue/units
α	Fractional order	$(0, 1]$ (dimensionless)
$\beta_H(t)$	Human infection rate	time-dependent (week^{-1})
$\beta_V(t)$	Mosquito infection rate	time-dependent (week^{-1})
σ_H	Incubation rate in humans	0.1–0.5 week^{-1} (∼2–10 days)
γ_H	Recovery rate in humans	0.05–0.3 week^{-1} (∼3–20 days)
μ_H	Human natural mortality rate	0.0002–0.001 week^{-1}
μ_V	Mosquito mortality rate	0.03–0.15 week^{-1} (∼7–23 days)
S_0, E_0, I_0, R_0	Initial human fractions	$[0, 1]$, $S_0 + E_0 + I_0 + R_0 = 1$
S_{v0}, I_{v0}	Initial mosquito fractions	$[0, 1]$, $S_{v0} + I_{v0} = 1$

2.1 FPINN Approximation Framework

Each compartment is approximated using a neural network

$$\hat{U}(t, \mathbf{x}; \theta) = (\hat{S}, \hat{E}, \hat{I}, \hat{R}, \hat{S}_v, \hat{I}_v),$$

where $t \in [0, 1]$ is normalized time, $\mathbf{x}$ denotes the environmental covariates, and θ represents trainable parameters. In addition, separate neural sub-networks are employed to estimate the time-varying transmission rates $\beta_H(t, \mathbf{x})$ and $\beta_V(t, \mathbf{x})$ from the same environmental covariates.

Physics-Informed Neural Networks: From PINN to FPINN Physics-Informed Neural Networks (PINNs) integrate physical laws as soft constraints during neural network training. The standard PINN approach for ODEs/PDEs minimizes:

$$\mathcal{L}_{\text{PINN}} = \mathcal{L}_{\text{data}} + \lambda \mathcal{L}_{\text{physics}},$$

where $\mathcal{L}_{\text{physics}}$ penalizes violations of differential equations at collocation points. Fractional PINNs (FPINNs) extend this framework to fractional differential equations (FDEs).

Loss Function and Physical Constraints The proposed FPINN optimizes a composite loss combining data fidelity, physical consistency, and temporal smoothness:

$$\mathcal{L} = \underbrace{\mathcal{L}_{\text{data}}}_{\text{Data fit}} + \underbrace{\lambda_{\text{phys}} \mathcal{L}_{\text{phys}}}_{\text{Physics}} + \underbrace{0.002 \mathcal{L}_{\text{smooth}}}_{\text{Smoothness}}, \tag{4}$$

where each component serves a distinct purpose.

Data Loss: Matches predicted incidence to observed cases via a robust combination:

$$\mathcal{L}_{\text{data}} = 0.6 \|\hat{I} - I_{\text{obs}}\|_2^2 + 0.3 \|\hat{I} - I_{\text{obs}}\|_1 + 0.1 \mathcal{L}_{\text{Huber}}(\hat{I}, I_{\text{obs}}), \tag{5}$$

where the Huber loss $\mathcal{L}_{\text{Huber}}(a, b) = \begin{cases} \frac{1}{2}(a-b)^2 & |a-b| \leq \delta, \\ \delta(|a-b| - \frac{1}{2}\delta) & \text{otherwise,} \end{cases}$ with $\delta = 1.0$ provides robustness to outliers.

ICCS Camera Ready Version 2026
To cite this paper please use the final published version:
DOI: 10.1007/978-3-032-29912-3_30

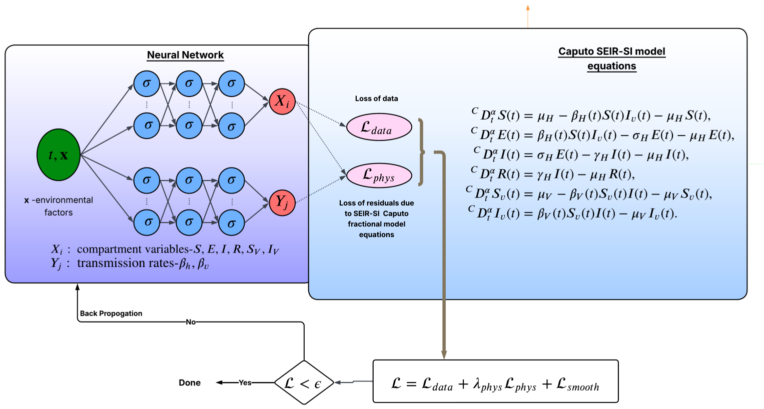

Fig. 1. Flow diagram of the proposed FPINN for SEIR-SI fractional dengue transmission model.

Algorithm 1 Fixed Fractional-Order Ensemble FPINN Training

Input: Observed dengue cases $\{I_{\text{obs}}(t_n)\}_{n=1}^N$, environmental features $\mathbf{x}(t_n)$, time grid $\{t_n\}_{n=1}^N$, fixed fractional orders $\mathcal{A}$
Output: Ensemble prediction $\bar{I}_H(t)$ and uncertainty estimates
1: **for** each $\alpha_m \in \mathcal{A}$ **do**
2: Generate a bootstrap sample from the training data
3: Initialize FPINN parameters
4: **while** not converged **do**
5: Predict SEIR–SI state variables and transmission rates using forward pass.
6: Approximate Caputo derivatives via L1 scheme
7: Compute composite loss
8: Update network parameters
9: **end while**
10: **end for**
11: Compute ensemble mean: $\bar{I}_H(t_n) = \frac{1}{|\mathcal{A}|}\sum_{\alpha_m \in \mathcal{A}} I_H^{(m)}(t_n)$
12: **return** $\bar{I}_H(t)$ and ensemble-based uncertainty

Physics Loss: Enforces fractional SEIR–SI dynamics through residuals:

$$\mathcal{R}_S = {}^C D_t^\alpha \hat{S} - (\mu_H - \beta_H \hat{S}\hat{I}_v - \mu_H \hat{S}), \tag{6a}$$
$$\mathcal{R}_E = {}^C D_t^\alpha \hat{E} - (\beta_H \hat{S}\hat{I}_v - \sigma_H \hat{E} - \mu_H \hat{E}), \tag{6b}$$
$$\mathcal{R}_I = {}^C D_t^\alpha \hat{I} - (\sigma_H \hat{E} - \gamma_H \hat{I} - \mu_H \hat{I}), \tag{6c}$$
$$\mathcal{R}_R = {}^C D_t^\alpha \hat{R} - (\gamma_H \hat{I} - \mu_H \hat{R}), \tag{6d}$$
$$\mathcal{R}_{S_v} = {}^C D_t^\alpha \hat{S}_v - (\mu_V - \beta_V \hat{S}_v \hat{I} - \mu_V \hat{S}_v), \tag{6e}$$
$$\mathcal{R}_{I_v} = {}^C D_t^\alpha \hat{I}_v - (\beta_V \hat{S}_v \hat{I} - \mu_V \hat{I}_v), \tag{6f}$$

ICCS Camera Ready Version 2026
To cite this paper please use the final published version:
DOI: 10.1007/978-3-032-29912-3_30

$$\mathcal{L}_{\text{phys}} = \frac{1}{N}\sum_{n=1}^{N}\left(\mathcal{R}_S^2 + \mathcal{R}_E^2 + \mathcal{R}_I^2 + \mathcal{R}_R^2 + \mathcal{R}_{S_v}^2 + \mathcal{R}_{I_v}^2\right). \tag{7}$$

Smoothness Regularization: Promotes temporally coherent predictions:

$$\mathcal{L}_{\text{smooth}} = \frac{1}{N-1}\sum_{n=2}^{N}\|\hat{I}(t_n) - \hat{I}(t_{n-1})\|_2^2. \tag{8}$$

Adaptive Weighting: The physics weight λ_{phys} decays exponentially during training:

$$\lambda_{\text{phys}}(epoch) = \lambda_0 e^{-\gamma \cdot epoch}, \tag{9}$$

where $\lambda_0 \in [0.05, 1.0]$ and $\gamma \in [0.05, 0.07]$ are tunable hyperparameters selected via validation. This strategy prioritizes physical consistency early in training while transitioning to data fitting in later epochs. The overall FPINN workflow, integrating data-driven learning with fractional SEIR–SI physics regularization, is summarized in Fig. 1 and Algorithm 2.1.

2.2 Data Collection

Weekly dengue case data and environmental variables were obtained from the San Juan, Puerto Rico, dengue dataset. The dataset was consisting of 936 weekly observations and 20 climate-related features [4]. Weekly dengue incidence was used as the response variable, and only numerical features were retained for modeling.

2.3 Implementation Details

Software: Python 3.8 version with PyTorch 2.0, NumPy, and scikit-learn libraries were used in the implementation of the proposed model.

Hyperparameters: Key hyperparameters are summarized in Table 2.

Training Configuration. Training was performed for a maximum of 200 epochs with early stopping (patience = 40). Gradient clipping (norm = 1.0) and dropout (10%) were applied for stability. The proposed model is computationally efficient; all experiments were conducted on a standard workstation, requiring approximately 30 minutes for training the full ensemble of five models and generating ensemble plots (about 6 minutes per individual model). While the ensemble approach introduces additional computational cost compared to a single model, the training can be parallelized and provides improved robustness and uncertainty estimation, justifying the moderate overhead. The proposed model was also evaluated against three baseline time series models commonly used in disease forecasting. These are:

1. **Standard FPINN**: Integer-order FPINN with fixed $\alpha = 1$.
2. **LSTM**: A three-layer bidirectional LSTM with 128 hidden units.
3. **TCN**: Temporal Convolutional Network with dilated convolutions.

ICCS Camera Ready Version 2026
To cite this paper please use the final published version:
DOI: 10.1007/978-3-032-29912-3_30

Table 2. FPINN hyperparameters and their values

Parameter	Value/Range
Hidden layers	3 residual blocks
Hidden units per layer	192
Activation function	tanh (encoder), softplus (outputs)
Learning rate (η)	0.0015 (AdamW)
Weight decay	1×10^{-6}
Batch size	1 (sequential processing)
Maximum epochs	200
Early stopping patience	40
λ_{phys} schedule	$\lambda_0 e^{-\gamma \cdot \text{epoch}}$
λ_0 range	$[0.05, 1.0]$ (learned)
γ range	$[0.05, 0.07]$ (learned)
λ_{smooth}	0.002 (fixed)
Time step Δt	1/52 (weekly discretization)
History length (L1)	104 steps (∼2 years)
Ensemble size (M)	5
Bootstrap rate	85%

Hyperparameter selection. All hyperparameters were determined using only the training and validation sets. The loss function weights (MSE 0.6, MAE 0.3, Huber 0.1, smoothness 0.002) were examined via sensitivity analysis: each weight was varied by factors of 0.5 and 1.5 while keeping the others constant, and validation MAE was monitored for a representative fractional order ($\alpha = 0.90$). Validation MAE changed by less than 10% for all variations except when the smoothness weight was doubled, confirming robustness. A grid search over hidden dimensions $\{128, 192, 256\}$ and residual blocks $\{2, 3, 4\}$ was conducted using the same α. The best single-α configuration (128 hidden units, 3 blocks) achieved a validation MAE of 2.86 and $R^2 = 0.926$. However, because the final model is an ensemble of five fractional orders ($\alpha = 0.80, \ldots, 1.00$), the two candidate architectures were evaluated on the full ensemble. The original architecture (192 hidden units, 3 blocks) produced an ensemble that improved over its best individual member (validation ensemble MAE 2.57 vs. best individual 2.85), whereas the 128×3 architecture did not (ensemble MAE 3.42 vs. best individual 2.86). Since the main goal of this work is to build an ensemble that demonstrates improved performance over individual models, the original architecture was kept unchanged.

3 Results and Simulations

This section provides an overall experimental analysis of the proposed system with an ensemble of fixed fractional orders. Each of the experiments follows the same set of data, preprocessing pipeline, and network architecture to make sure

ICCS Camera Ready Version 2026
To cite this paper please use the final published version:
DOI: 10.1007/978-3-032-29912-3_30

that the observed differences are only due to the treatment of the fractional order and ensemble construction.

3.1 Quantitative Performance

The proposed model, as compared to baseline time series models (see Table 3), achieves a 36.2% reduction in MAE relative to the TCN(Temporal Convolutional Network) model and a 29.1% reduction compared to the LSTM(Long Short-Term Memory) model. In addition, the ensemble improves MAE by 13.9% over the integer-order FPINN ($\alpha = 1$) and 6.7% improvement over the best fractional order FPINN ($\alpha = 0.95$). These results show that incorporating fractional-order memory within a physics-informed ensemble framework leads to more accurate and robust dengue incidence predictions than both purely data-driven models and integer-order physics-informed counterparts. The FPINN also exhibits a very small train–test performance gap (see Table 4), indicating superior generalization and robustness to distribution shifts compared to other baseline methods.

Table 3. Test set performance comparison with baseline models.

Model	MAE	RMSE	R^2
FPINN Ensemble	**6.25**	**11.03**	**0.8956**
Best FPINN ($\alpha = 0.95$)	6.70	11.32	0.8900
Standard FPINN ($\alpha = 1$)	7.26	13.11	0.8525
LSTM	8.81	13.52	0.8412
TCN	9.80	15.17	0.8003

Table 4. Generalization performance across models.

Model	Train R^2	Test R^2	Drop
FPINN Ensemble (fixed α)	0.9640	0.8956	6.8%
Best FPINN ($\alpha = 0.95$)	0.9489	0.8900	5.9%
Standard FPINN ($\alpha = 1$)	0.9593	0.8525	10.7%
LSTM	0.9363	0.8412	9.5%
TCN	0.9476	0.8003	14.7%

3.2 Fractional-Order Ensemble Design

Five independent FPINN models are trained with pre-defined Caputo fractional orders $\alpha \in \{0.80,\ 0.85,\ 0.90,\ 0.95,\ 1.00\}$, where $\alpha = 1.00$ corresponds to the integer-order FPINN.

Remark 1. The fractional order α is considered here as a fixed hyperparameter rather than a learnable parameter to ensure the numerical stability and consistent convergence throughout the training process. The Joint optimization of

ICCS Camera Ready Version 2026
To cite this paper please use the final published version:
DOI: 10.1007/978-3-032-29912-3_30

fractional order α and network weights, along with other model parameters, causes an ill-conditioned inverse problem since the fractional derivative operator is non-linearly coupled with the solution history, which often results in flat or unstable gradients. To overcome this issue, an ensemble of FPINN models with distinct, pre-specified α values was proposed.

At inference time, predictions are combined pointwise using simple averaging. Predictive uncertainty is quantified using the ensemble standard deviation.

Table 5 reports the performance of individual fixed-α models across training, validation, and test sets.

Table 5. Performance of pre-specified α FPINN models across datasets

α	**Training**			**Validation**			**Test**		
	MAE	RMSE	R^2	MAE	RMSE	R^2	MAE	RMSE	R^2
0.80	5.87	13.75	0.9438	2.85	3.70	0.9182	9.71	20.26	0.6478
0.85	7.45	19.68	0.8848	3.05	3.89	0.9095	7.03	15.49	0.7942
0.90	6.79	16.40	0.9201	3.83	5.35	0.8292	7.49	12.84	0.8586
0.95	6.82	13.11	0.9489	3.82	4.82	0.8613	**6.70**	**11.32**	**0.8900**
1.00	5.04	11.71	0.9593	3.28	4.44	0.8825	7.26	13.11	0.8525

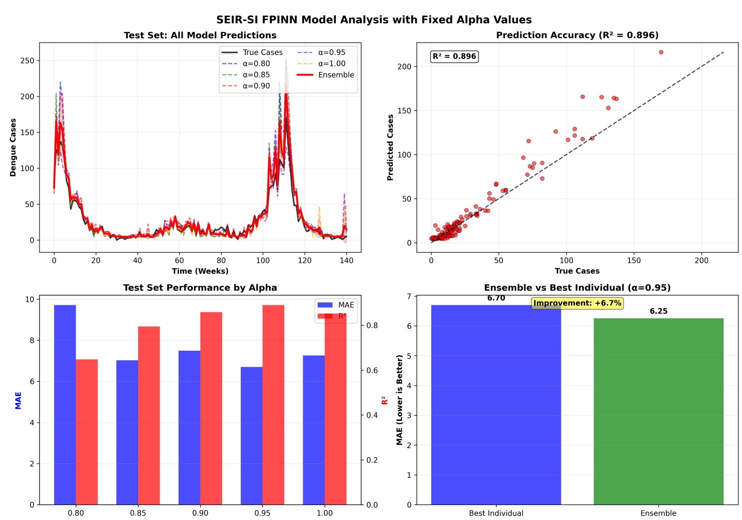

Fig. 2. Test-set performance of the fixed-α SEIR–SI FPINN. The ensemble consistently improves prediction accuracy over individual models, achieves $R^2 = 0.896$, and reduces MAE relative to the best single fractional order ($\alpha = 0.95$).

ICCS Camera Ready Version 2026
To cite this paper please use the final published version:
DOI: 10.1007/978-3-032-29912-3_30

Moderate fractional orders ($\alpha \approx 0.90$–0.95) consistently perform better than both the lower fractional orders and the integer-order model, which shows the benefit of incorporating memory effects into dengue transmission modeling. Fig. 2 provides an overall evaluation of the proposed framework on the test dataset. The ensemble closely follows the observed dengue dynamics in time and achieves strong agreement with observed cases ($R^2 = 0.896$), and also performs better than individual fixed-α models. Fig. 3 presents predicted versus observed dengue cases for all individual FPINN models and the corresponding ensemble. Individual models show increasing dispersion at higher incidence levels, particularly for extreme fractional orders, whereas the ensemble predictions are more tightly aligned with the identity line.

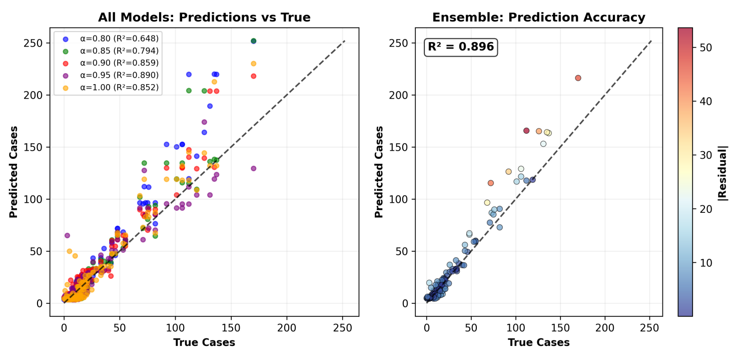

Fig. 3. Predicted versus observed dengue cases for fixed-α FPINN models and the ensemble on the test set.

3.3 Ensemble Performance and Generalization

Table 6 summarizes the predictive accuracy and uncertainty characteristics of the proposed model on the test dataset. The ensemble outperforms the best individual model by 6.7%. Uncertainty estimates show the low median values during stable transmission periods while having higher variability during epidemic peaks, reflecting the increased model disagreement when incidence changes rapidly. Overall, these results suggest that the ensemble provides both improved predictive accuracy and meaningful uncertainty quantification, which can enhance the reliability of epidemic forecasts.

Fig. 4 compares the ensemble model to the best single model. The ensemble more accurately predicts outbreak peaks and has fewer large errors, improving overall accuracy by 6.7%, and was performing better than the individual model two-thirds of the time, which shows that combining models creates a more robust predictor.

ICCS Camera Ready Version 2026
To cite this paper please use the final published version:
DOI: 10.1007/978-3-032-29912-3_30

Table 6. Ensemble Uncertainty Quantification (Test Set)

Metric	Value	Description
Predictive Performance		
Ensemble MAE	6.25	Mean absolute error
Ensemble RMSE	11.03	Root mean square error
Ensemble R^2	0.896	Coefficient of determination
Best MAE ($\alpha = 0.95$)	6.70	Best single model
Worst MAE ($\alpha = 0.80$)	9.71	Worst single model
Improvement	+6.7%	Ensemble gain
Predictive Uncertainty		
Mean $\sigma_I(t)$	5.81	Average uncertainty
Median $\sigma_I(t)$	3.17	Median uncertainty
Max $\sigma_I(t)$	45.32	Peak uncertainty
Min $\sigma_I(t)$	0.12	Stable-period uncertainty
Std $\sigma_I(t)$	5.85	Uncertainty variability

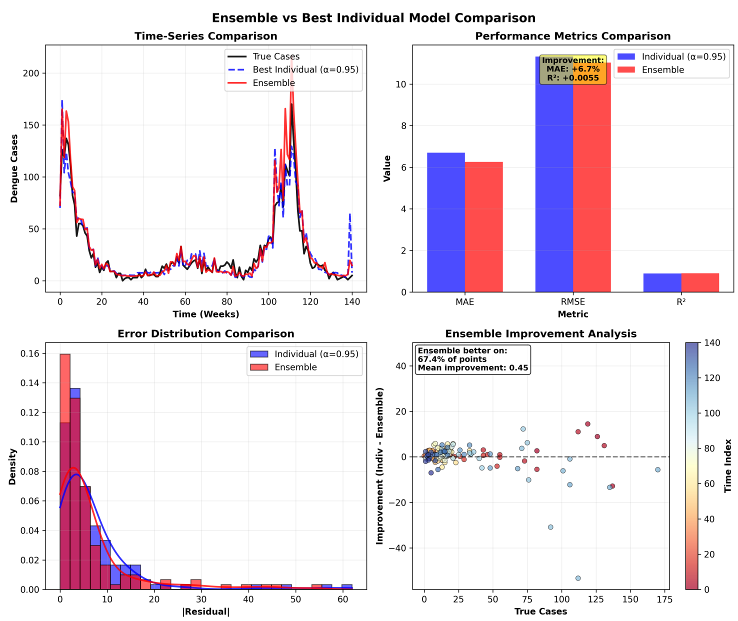

Fig. 4. Comparison between the fixed-α ensemble and the best individual model ($\alpha = 0.95$). The ensemble more accurately captures epidemic peaks, reduces error dispersion, and achieves improved predictive accuracy, outperforming the individual model on the majority of test time points.

Fig. 5 illustrates that model performance is sensitive to the fractional order α. While α values near 0.90–0.95 perform best, the optimal α differed across

ICCS Camera Ready Version 2026
To cite this paper please use the final published version:
DOI: 10.1007/978-3-032-29912-3_30

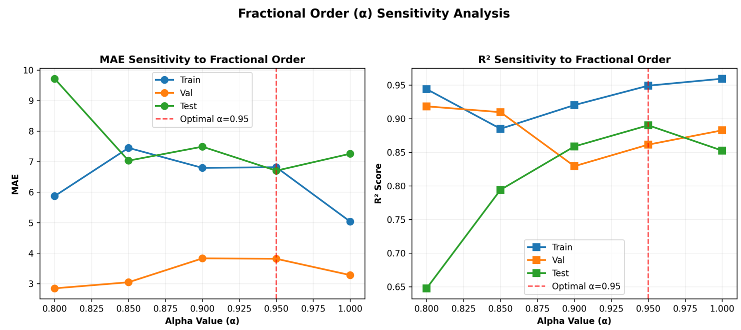

Fig. 5. Sensitivity of model performance to the fractional order α. Variation of MAE (left) and R^2 (right) across training, validation, and test sets shows a non-monotonic dependence on α, with moderate fractional orders ($\alpha \approx 0.90$–0.95) yielding the best generalization performance.

the datasets. This lack of a single best α further justifies the ensemble method, which aggregates predictions from a range of α values to improve the robustness.

4 Discussion and Conclusion

This paper shows that the combination of fractional calculus and physics-informed neural networks provides a powerful and meaningful tool for dengue disease transmission modeling. The proposed FPINN model relaxes the Markovian property implicitly present in traditional compartmental models and captures the long-range memory effects that are naturally inherent in vector-borne diseases. The use of fixed fractional orders promotes stable training, and the ensemble approach combines different memory regimes to improve robustness and uncertainty estimation.

Across all the datasets, the FPINN ensemble averaging outperforms the individual fixed-α models and data-driven baselines. On the test set, the ensemble achieves a 6.7% reduction in MAE over the best individual model ($\alpha = 0.95$) and shows strong generalization with an R^2 of 0.896. Uncertainty estimates remain low during stable transmission periods and increase during outbreak peaks, which reflects meaningful model disagreement rather than the numerical instability. This behavior indicates that the ensemble can provide both accurate predictions and reliable uncertainty information, which is essential for epidemiological decision-making.

Several limitations remain. In the proposed formulation, the assumption of a homogeneous population is considered, and does not explicitly model either the spatial structure or multi-strain interactions. Besides this, though the Caputo L1 scheme is efficient on the time horizon under investigation, longer datasets might pose a problem due to the computational efficiency of this scheme. These areas can be covered in future work. In addition, the applicability of the pro-

ICCS Camera Ready Version 2026
To cite this paper please use the final published version:
DOI: 10.1007/978-3-032-29912-3_30

posed framework to other diseases may require modifications to the compartmental structure, as the SEIR–SI model is tailored for vector-borne transmission. Moreover, the present study is limited to a single dengue dataset; therefore, future work will also focus on evaluating the proposed framework across multiple datasets and extending it to other infectious diseases to further enhance its generalizability and robustness.

Finally, the proposed framework addresses the key gaps identified in the introduction by integrating fractional-order dynamics with physics-informed learning, enabling data-driven time-varying transmission modeling, and employing an ensemble of fractional orders to improve robustness and uncertainty estimation. In conclusion, the findings suggest that the use of fractional physics-informed learning can be a credible concept in epidemic prediction. The proposed FPINN ensemble is more accurate and interpretable because memory effects have been introduced by using fractional operators and enforced mechanistic structure by requiring SEIR-SI dynamics. These hybrid models can be a promising way to create coherent early-warning systems and data-driven planning for public health.

Acknowledgments

This research was supported by the Science and Engineering Research Board (SERB), under the Mathematical Research Impact Centric Support (MATRICS) grant, Project No. MTR/2023/001395.

References

1. Agbata, B.C., Kovaci, S., Agbebaku, D.F., et al.: Fractional-order model of malaria incorporating treatment and prevention strategies. Scientific Reports **15**, 29290 (2025). https://doi.org/10.1038/s41598-025-14280-w
2. Aguiar, M., Anam, V., Blyuss, K.B., Estadilla, C.D.S., Guerrero, B.V., Knopoff, D., Kooi, B.W., Srivastav, A.K., Steindorf, V., Stollenwerk, N.: Mathematical models for dengue fever epidemiology: A 10-year systematic review. Physics of Life Reviews **40**, 65–92 (2022). https://doi.org/10.1016/j.plrev.2022.02.001
3. Diethelm, K.: The analysis of fractional differential equations: An application-oriented exposition using differential operators of Caputo type. Springer Science & Business Media (2010)
4. DrivenData: Dengai: Predicting disease spread. https://www.drivendata.org/competitions/44/dengai-predicting-disease-spread/ (2016), accessed: 2025-01-16
5. Esteva, L., Vargas, C.: Analysis of a dengue disease transmission model. Mathematical Biosciences **150**(2), 131–151 (1998). https://doi.org/https://doi.org/10.1016/S0025-5564(98)10003-2
6. Harjule, P., Harshit, Kumar, R.: A hybrid integer–caputo fractional order dengue transmission model: Parameter optimization and empirical study with real-world data. Mathematics and Computers in Simulation **243**, 339–361 (2026). https://doi.org/10.1016/j.matcom.2025.11.040

ICCS Camera Ready Version 2026
To cite this paper please use the final published version:
DOI: 10.1007/978-3-032-29912-3_30

7. Kheiri, H., Jafari, M.: Stability analysis of a fractional order model for the hiv/aids epidemic in a patchy environment. Journal of Computational and Applied Mathematics **346**, 323–339 (2019). https://doi.org/10.1016/j.cam.2018.06.055
8. Li, C., Zeng, F.: Numerical Methods for Fractional Calculus. Chapman and Hall/CRC, New York (2015). https://doi.org/10.1201/b18503
9. Messina, J.P., Brady, O.J., Golding, N., Kraemer, M.U., Wint, G.W., Ray, S.E., Pigott, D.M., Shearer, F.M., Johnson, K., Earl, L., et al.: The current and future global distribution and population at risk of dengue. Nature microbiology **4**(9), 1508–1515 (2019). https://doi.org/https://doi.org/10.1038/s41564-019-0476-8
10. Millevoi, C., Cozzo, G., Pischiutta, M.: A physics-informed neural network approach for compartmental epidemiological models. PLOS Computational Biology **20**(9), e1012387 (2024). https://doi.org/https://doi.org/10.1371/journal.pcbi.1012387
11. Ogunlade, S.T., Meehan, M.T., Adekunle, A.I., McBryde, E.S.: A systematic review of mathematical models of dengue transmission and vector control: 2010–2020. Viruses **15**(1), 254 (2023). https://doi.org/10.3390/v15010254
12. Pang, G., Lu, L., Karniadakis, G.E.: fpinns: Fractional physics-informed neural networks. SIAM Journal on Scientific Computing **41**(4), A2603–A2626 (2019). https://doi.org/10.1137/18M1229845
13. Podlubny, I.: Fractional differential equations. Academic press (1999)
14. Raissi, M., Perdikaris, P., Karniadakis, G.E.: Physics-informed neural networks: A deep learning framework for solving forward and inverse problems involving nonlinear partial differential equations. Journal of Computational Physics **378**, 686–707 (2019). https://doi.org/doi:10.1016/j.jcp.2018.10.045
15. Sardar, T., Rana, S., Chattopadhyay, J.: A mathematical model of dengue transmission with memory. Communications in Nonlinear Science and Numerical Simulation **22**(1–3), 511–525 (2015). https://doi.org/10.1016/j.cnsns.2014.08.009
16. Shaier, S., Raissi, M., Seshaiyer, P.: Data-driven approaches for predicting spread of infectious diseases through DINNs: Disease informed neural networks. arXiv preprint (2021). https://doi.org/10.48550/arXiv.2110.05445
17. Sikder, A.K., Islam, M.H.: Fractional order modeling of dengue transmission dynamics in bangladesh. Partial Differential Equations in Applied Mathematics **14**, 101150 (2025). https://doi.org/10.1016/j.padiff.2025.101150
18. Ullah, S., Khan, M.A., Farooq, M.: A new fractional model for the dynamics of the hepatitis b virus using the caputo–fabrizio derivative. European Physical Journal Plus **133**, 237 (2018). https://doi.org/10.1140/epjp/i2018-12072-4
19. World Health Organization: Dengue and severe dengue (2023), available: https://www.who.int/news-room/fact-sheets/detail/dengue-and-severe-dengue
20. Zinihi, A.: Identifying memory effects in epidemics via a fractional SEIRD model and physics-informed neural networks. arXiv preprint (2025). https://doi.org/https://arxiv.org/abs/2509.22760

ICCS Camera Ready Version 2026
To cite this paper please use the final published version:
DOI: 10.1007/978-3-032-29912-3_30